

Investigation of MAX phase/c-BN composites

Tokoloho Rampai^{a,b}, C.I. Lang^{a,*}, Iakovos Sigalas^{b,c}

^aCentre for Materials Engineering, Department of Mechanical Engineering, University of Cape Town, Cape Town, South Africa.

^bDST/NRF Centre of Excellence in Strong Materials, University of the Witwatersrand, Johannesburg, South Africa

^cSchool of Chemical and Metallurgical Engineering, University of the Witwatersrand, Johannesburg, South Africa

Received 17 August 2012; received in revised form 31 October 2012; accepted 31 October 2012

Available online 11 January 2013

Abstract

We have successfully fabricated novel MAX phase/c-BN composite materials, which have the potential to improve significantly on current grinding and cutting materials. The synthesis conditions include elevated temperatures and moderate pressure, which allows for good bonding of the carrier to the abrasive. Preliminary results show that MAX phase ceramics offer outstanding benefits as carrier materials for c-BN abrasive particles.

© 2012 Elsevier Ltd and Techna Group S.r.l. All rights reserved.

Keywords: B. Composites; E. Cutting tools; c-BN; MAX phases

1. Introduction

Current backing materials in grinding and cutting tools are either ceramics or metals; however ceramics have the disadvantage of low toughness, and many metals have the disadvantages of high density and intolerance to extreme temperatures. The utilization of composite cutting materials, in which hard abrasive particles are embedded in a softer carrier material, is currently limited by the properties of the available carrier materials. Carrier materials which are soft can lose cutting efficiency as the abrasive particles are lost or alternatively penetrate the carrier; those which are hard may suffer loss of abrasive through fracture; metallic carrier materials commonly experience high friction with the work piece; and the bonding between carrier material and abrasive may be insufficient, resulting in reduced processing power of the cutting tool [1].

MAX phase ceramics have both metallic and ceramic properties [1]; they are relatively ductile and machinable, yet also heat-tolerant, strong and lightweight [2,3]. They accordingly have unique potential as carrier materials for

abrasive media such as cubic boron nitride (c-BN), a widely used abrasive in cutting tools which is exceeded in hardness only by diamond [4,5]. Composites of MAX phase ceramics with c-BN may thus offer outstanding advantages in the tooling industry.

MAX phases are carbide and nitride ternary ceramics with the general formula $M_{n+1}AX_n$, where M=early transition metal; A=group A element, usually IIIA or IVA; X=C or N;

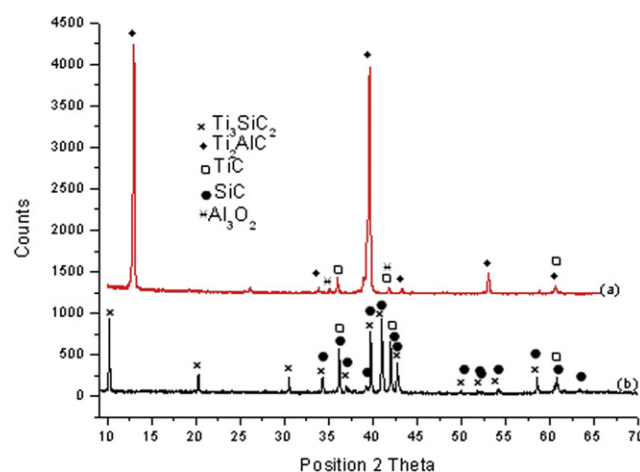


Fig. 1. X-ray diffractogram of: (a) Ti_2AlC and (b) Ti_3SiC_2 , synthesized at 1400 °C, 30 MPa, 120 min.

*Corresponding author. Current address: Department of Engineering, Macquarie University, NSW 2109, Australia. Tel.: +61 298509149; fax: +61 298509128.

E-mail address: candace.lang@gmail.com (C.I. Lang).

and n is 1, 2 or 3 [6]. The most widely investigated are Ti_2AlC (M_2AX phase) and Ti_3SiC_2 (M_3AX_2 phase): both materials possess a combination of excellent mechanical properties, electrical and thermal conductivities higher than those of pure Ti, and good resistance to both oxidation and thermal shock [1,7]. Relative to conventional ceramics, MAX phase ceramics offer enhanced fracture toughness and reduced hardness [8].

The MAX phase ceramics decompose between 850 °C and 2300 °C at ambient pressure [2,9,10], depending on the type and number of impurities present. The synthesis of c-BN/MAX phase composites would require similarly high temperatures, because the strong covalent bonds of c-BN can only be rearranged in high temperature interaction processes. The synthesis of MAX phase/c-BN composites thus presents a challenge in that the materials must react together at elevated temperatures, without allowing decomposition of the MAX phase and the associated degradation of properties. The aim of the work presented here is to determine the optimum conditions for reacting these two materials, to evaluate the nature of the reaction at these temperatures, to identify any interfacial phases which form, to synthesize a MAX phase/c-BN composite and to investigate whether the mechanical behavior offers improvements over current cutting tool materials.

2. Materials and methods

Ti_2AlC and Ti_3SiC_2 MAX phase materials were synthesized from the following powders: titanium (44 μm , 99%), aluminum (44 μm , 99.97%), activated carbon (13.2 μm , 99%) and silicon carbide (44 μm , 99%). A stoichiometric combination of the powders was mixed and milled by planetary ball mill for 6 h in hexane, in a zirconium milling pot, at 300 rpm. The dried powders were hot-press sintered at 1400 °C for 120 min at 30 MPa pressure. The sintered samples were notched, then fractured into two pieces by a three-point bend jig, for characterization of fracture surfaces. Sintered samples were analyzed by Archimedes' Method (density), Scanning Electron Microscopy (microstructure), Energy Dispersive Spectroscopy (composition), and X-Ray Diffraction (phase analysis). XRD diffractograms were collected using $\text{Cu(K}\alpha\text{)}$ radiation produced at 40 KV and 20 mA, over a 2θ range of 10°–90° using a 7 min, no spin profile for phase analysis.

Interaction between the synthesized MAX phases and c-BN was evaluated using reaction couples made from the polished MAX phase samples, sintered as described above, and a bulk (rather than particulate) commercial c-BN material, Amborite 90, containing approximately 90% c-BN (the remaining

Table 1
Density, porosity and phase composition of MAX phase samples sintered at 1400 °C, 30 MPa for 120 min.

MAX phase	Theoretical density (g/cm^3)	Measured density (g/cm^3)	Open porosity (%)	Phase composition (in order of prevalence)
Ti_2AlC	4.11	4.08	1.10	Ti_2AlC , TiC, Al_2O_3
Ti_3SiC_2	4.52	4.44	0.19	Ti_3SiC_2 , TiC, SiC

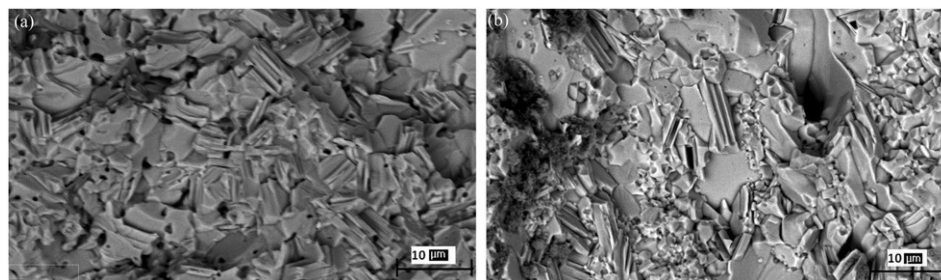


Fig. 2. SEM image showing platelet structure of fracture surface, (a) Ti_2AlC and (b) Ti_3SiC_2 .

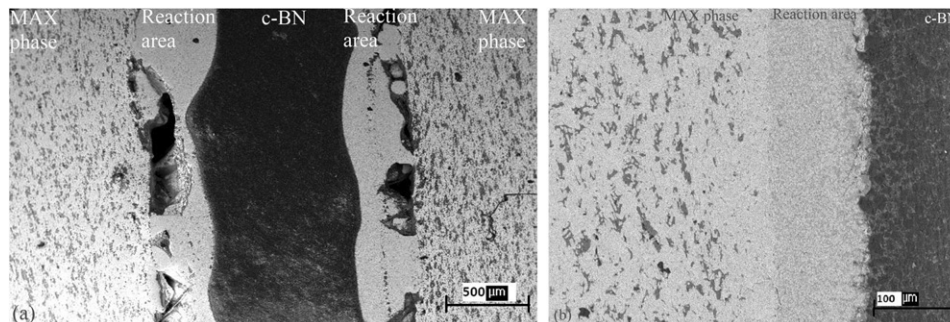


Fig. 3. BSE (CL) image of the reaction couple Ti_2AlC /c-BN reacted at 1500 °C for 30 min; (a) without applied pressure and (b) with 10 MPa pressure.

phases in the material are AlN and AlB₂). MAX phase/c-BN reaction couples were hot-press sintered in a graphite crucible at 1400 °C and 1500 °C for 30 min dwell time, at a pressure of 10 MPa or without applied pressure. The resulting couples were analyzed as described above.

For MAX phase/c-BN composite synthesis, sintered MAX phase ceramic (Ti₂AlC or Ti₃SiC₂) was crushed to < 20 μm powder. The MAX powder was then mixed with 8 μm c-BN powder in the ratio of 80:20 vol%,

MAX:c-BN, using a tubular mixer at 67 rpm for 4 h. The MAX/c-BN powder mixture was poured into a graphite pot, and then sintered in a spark plasma sintering apparatus (SPS). Sintering conditions were 1500 °C, 20 MPa for the Ti₂AlC composite; and 1400 °C, 20 MPa for the Ti₃SiC₂ composite; both for 10 min. The sintered composite samples were fractured into two pieces by a three-point bend jig after notching. One half was ground flat and polished to be used for SEM imaging of the cross-section,

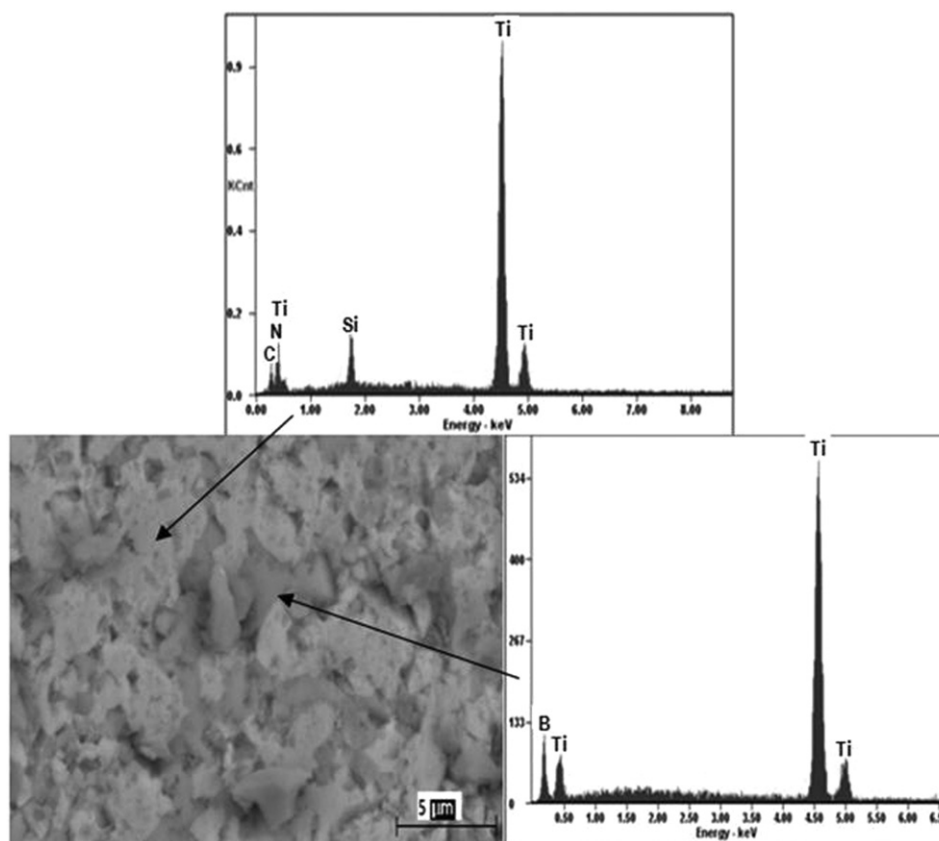


Fig. 4. BSE image with EDS analysis of the reaction zone from the reaction couple Ti₂AlC/c-BN reacted at 1500 °C, 10 MPa, 30 min.

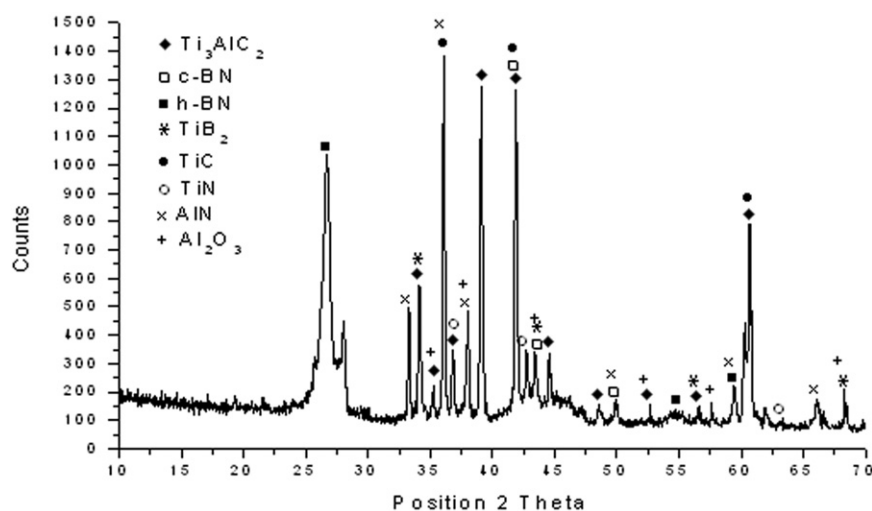


Fig. 5. X-ray diffractogram of the reaction couple Ti₂AlC/c-BN sintered at 1500 °C, 10 MPa, 30 min.

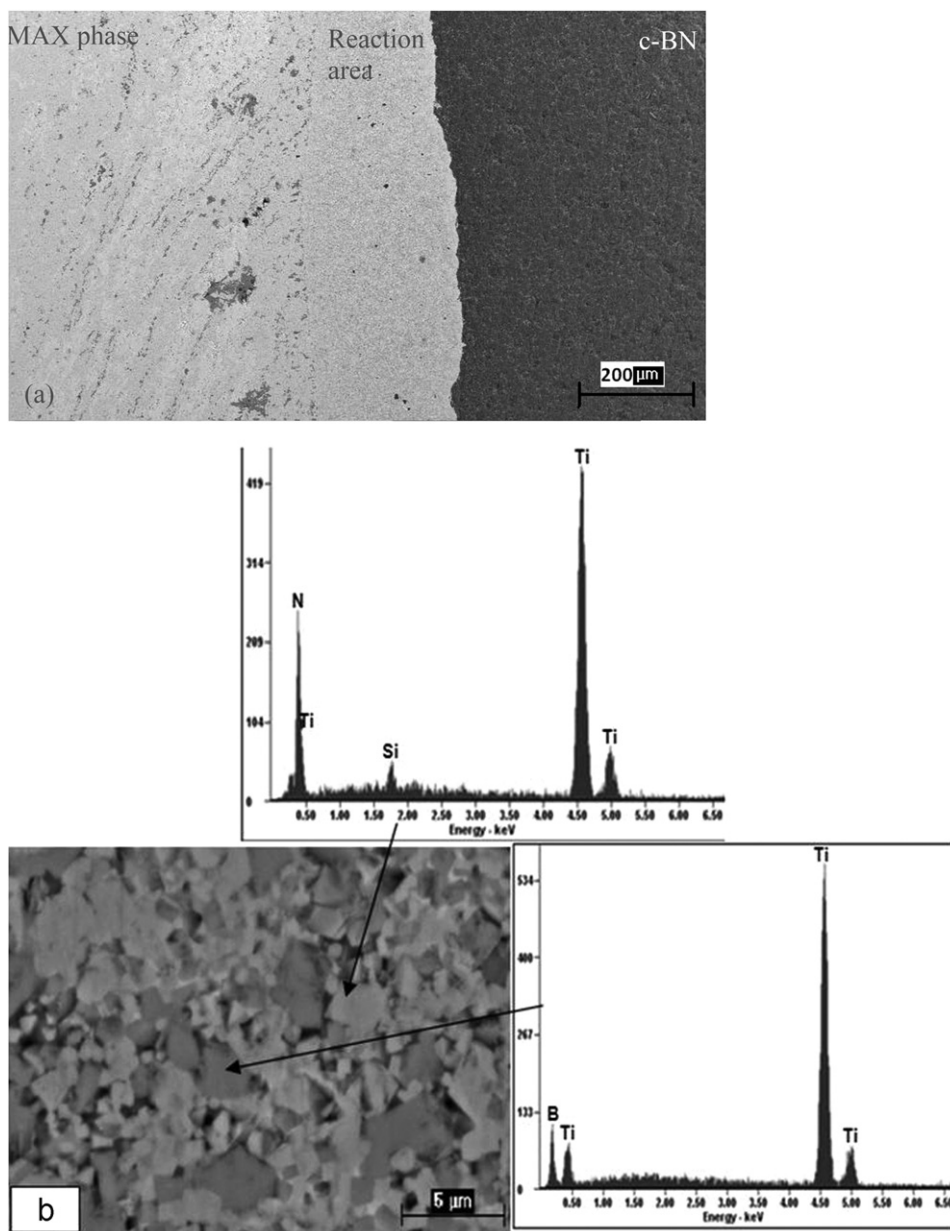


Fig. 6. (a) BSE (CL) image of the reaction couple $\text{Ti}_3\text{SiC}_2/\text{c-BN}$ reacted at 1400 $^{\circ}\text{C}$, 30 min and 10 MPa pressure, and (b) BSE image with EDS analysis of the reaction zone in (a).

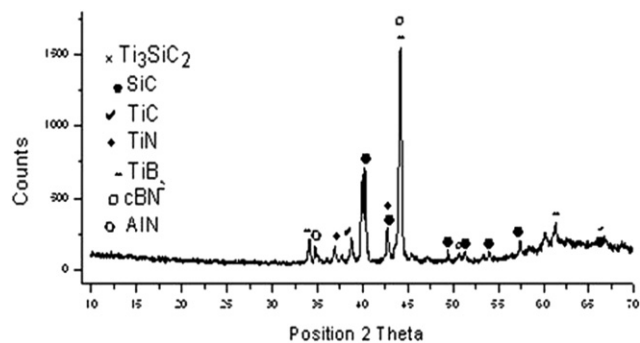


Fig. 7. X-ray diffractogram of the reaction couple $\text{Ti}_3\text{SiC}_2/\text{c-BN}$ reacted at 1400 $^{\circ}\text{C}$, 30 min and 10 MPa pressure.

from the surface of the sample to the core, to determine c-BN dispersion in the MAX phase and for EDS analysis. The other half was used to study the fracture surface.

3. Results

3.1. MAX phase synthesis and microstructure

Fig. 1 shows XRD measurements which confirm the majority phases in each sintered sample to be the MAX phases Ti_2AlC and Ti_3SiC_2 respectively. In the Ti_2AlC sample (Fig. 1a), small quantities of TiC and Al_2O_3 are observed, and in the Ti_3SiC_2 sample (Fig. 1b) SiC and TiC are present. The densities of the sintered MAX phases were

99.27% (Ti_2AlC) and 98.23% (Ti_3SiC_2) of the theoretical density, as shown in Table 1. Fig. 2a and b shows the fracture surfaces of sintered Ti_2AlC and Ti_3SiC_2 samples, revealing a grain size less than $10\text{ }\mu\text{m}$ and the platelet morphology characteristic of MAX phases [6]. The rough fracture surface and scarcity of cleavage surfaces is typical of ductile fracture, and is consistent with the reported high fracture toughness of the MAX phase materials [8].

3.2. Reaction couples

3.2.1. $\text{Ti}_2\text{AlC}/\text{c-BN}$ reaction couples:

Reaction of $\text{Ti}_2\text{AlC}/\text{c-BN}$ couples at $1400\text{ }^\circ\text{C}$ resulted in some interaction but no adhesion between the Ti_2AlC and c-BN. Further testing was carried out at $1500\text{ }^\circ\text{C}$. Fig. 3 shows SEM images of $\text{Ti}_2\text{AlC}/\text{c-BN}$ couples, reacted at $1500\text{ }^\circ\text{C}$ for 30 min (a) without pressure and (b) under an applied pressure of 10 MPa. Fig. 3a shows an irregular reaction zone between Ti_2AlC and c-BN with a thickness of approximately $400\text{ }\mu\text{m}$. Significant porosity is observed at the MAX phase/reaction zone interfaces; but not at the c-BN/reaction zone interfaces. The c-BN/reaction zone interface is seen to have roughened considerably in comparison to the flat surface of the c-BN before reaction. Fig. 3b shows that increasing the reaction pressure to 10 MPa resulted in a reduction in thickness of the reaction zone to about $100\text{ }\mu\text{m}$. The increased pressure also results in elimination of the porosity at the MAX phase/reaction zone interface; and a flat interface is now seen between the c-BN and the reaction zone, which is seen to be more uniform than in Fig. 3a.

Fig. 4 shows a SEM image with EDS analysis of the reaction zone between Ti_2AlC and c-BN reacted at 10 MPa, as shown above. This analysis reveals the presence of a light region containing Ti, C, Si and N (possible phases are TiC, SiC, TiN); and a darker phase containing Ti and B, (probably TiB_2). The SiC is probably surface contamination from the SiC grinding paper used in sample preparation, as there were no Si additions to the reaction couple and none was identified by XRD.

Fig. 5 shows an XRD diffractogram of a cross section of the reaction couple shown in Fig. 3b, including the MAX phase, c-BN and reaction zone. The Ti_2AlC peak is no longer evident as shown by comparison with Fig. 1a; Ti_3AlC_2 peaks are observed instead, suggesting that a transformation of Ti_2AlC to Ti_3AlC_2 (also a MAX phase)

has taken place. This is consistent with a previous report of a Ti_2AlC to Ti_3AlC_2 transformation at $1350\text{ }^\circ\text{C}$, by Zhu et al. [11]. A partial transformation of c-BN to h-BN has also occurred. Peaks showing secondary phases TiC, Al_2O_3 , AlN, TiN and TiB_2 are consistent with the EDS analysis of the reaction zone seen in Fig. 4. The same composition and phase results were seen for the $\text{Ti}_2\text{AlC}/\text{c-BN}$ couples reacted at $1500\text{ }^\circ\text{C}$ for 30 min without pressure; however the defects in this reaction zone, as seen in Fig. 3a, precluded further testing under these conditions.

3.2.2. $\text{Ti}_3\text{SiC}_2/\text{c-BN}$ reaction couples

The $\text{Ti}_3\text{SiC}_2/\text{c-BN}$ reaction couple was first heat treated at $1500\text{ }^\circ\text{C}$ without external load. The reaction couple showed no bonding interaction at all, the materials separating as soon as they were removed from the graphite pot. XRD analysis of the Ti_3SiC_2 sample after this heat treatment showed that it had undergone decomposition. Barsoum et al. [3] reported that the stability of MAX phases is sensitive to contamination by oxygen or other impurities; this may account for the decomposition observed here, as we were not able entirely to exclude oxygen in this work.

Lowering the temperature to $1400\text{ }^\circ\text{C}$ and applying 10 MPa pressure promoted the reaction of the MAX phase with c-BN, leading to adherence between the two components. Fig. 6a shows that these conditions resulted in a reaction zone of approximately $200\text{ }\mu\text{m}$ in thickness between the MAX phase and c-BN. Fig. 6b is an EDS

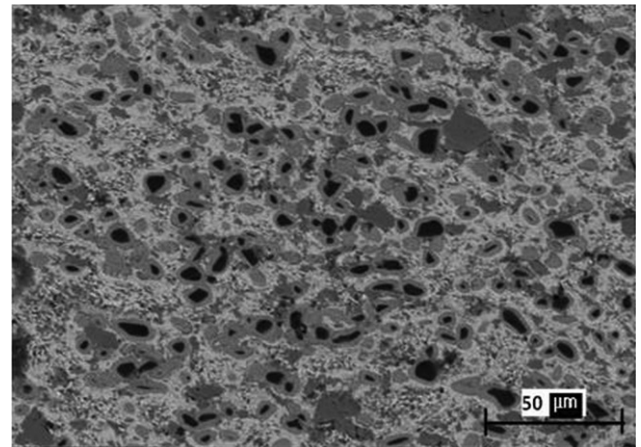


Fig. 8. SEM BSE image of sintered $\text{Ti}_2\text{AlC}/\text{c-BN}$ composite.

Table 2

Thickness and phase composition of the reaction zones of MAX phase/c-BN reaction couples sintered for 30 min under the conditions shown.

Reaction couple	Pressure (MPa)	1400 °C	Phase composition	1500 °C	Phase composition
		Reaction zone Thickness (μm)		Reaction zone Thickness (μm)	
$\text{Ti}_2\text{AlC}/\text{c-BN}/\text{Ti}_2\text{AlC}$	0	Not tested	TiB_2 , TiN, TiSi_2	400	TiB_2 , TiN, TiC
	10	No adhesion		100	TiB_2 , TiN, TiC
$\text{Ti}_3\text{SiC}_2/\text{c-BN}/\text{Ti}_3\text{SiC}_2$	0	Not tested		No adhesion	
	10	200		Not tested	

analysis of the reaction area in Fig. 6a: the darker phase contains Ti and B (probably TiB_2); and the lighter phase contains Ti, Si and N (probably TiN and TiSi_2). Fig. 7 shows the XRD results from the cross-section of the reaction couple shown in Fig. 6a, including the MAX phase, c-BN and reaction zone. It shows the presence of c-BN but not Ti_3SiC_2 , suggesting that decomposition of the MAX phase has occurred. Secondary phases TiC , TiSi and SiC (possibly decomposed MAX phase), AlN , AlB , TiN and TiB are also observed.

The reaction zone of the $\text{Ti}_3\text{SiC}_2/\text{c-BN}$ couple sintered at 1400°C is about twice the thickness of the $\text{Ti}_2\text{AlC}/\text{c-BN}$ couple sintered at 1500°C , both under pressure of 10 MPa. These two sintered couples showed interaction of MAX

phase/c-BN materials, with good adhesion and a uniform reaction zone. In both cases there was transformation of the starting MAX phase; both couples exhibited secondary phases of TiN , TiB_2 and TiC after reaction. Table 2 summarizes the results of the reaction experiments.

3.3. MAX phase/c-BN composites

MAX phase/c-BN composites have been synthesized previously under pressures in the GPa range at elevated temperatures [12]. In Sections 3.3.1 and 3.3.2, we show the results of MAX phase/c-BN composite synthesis at significantly lower pressures and similar or lower temperatures. Some alumina (Al_2O_3) contamination was observed

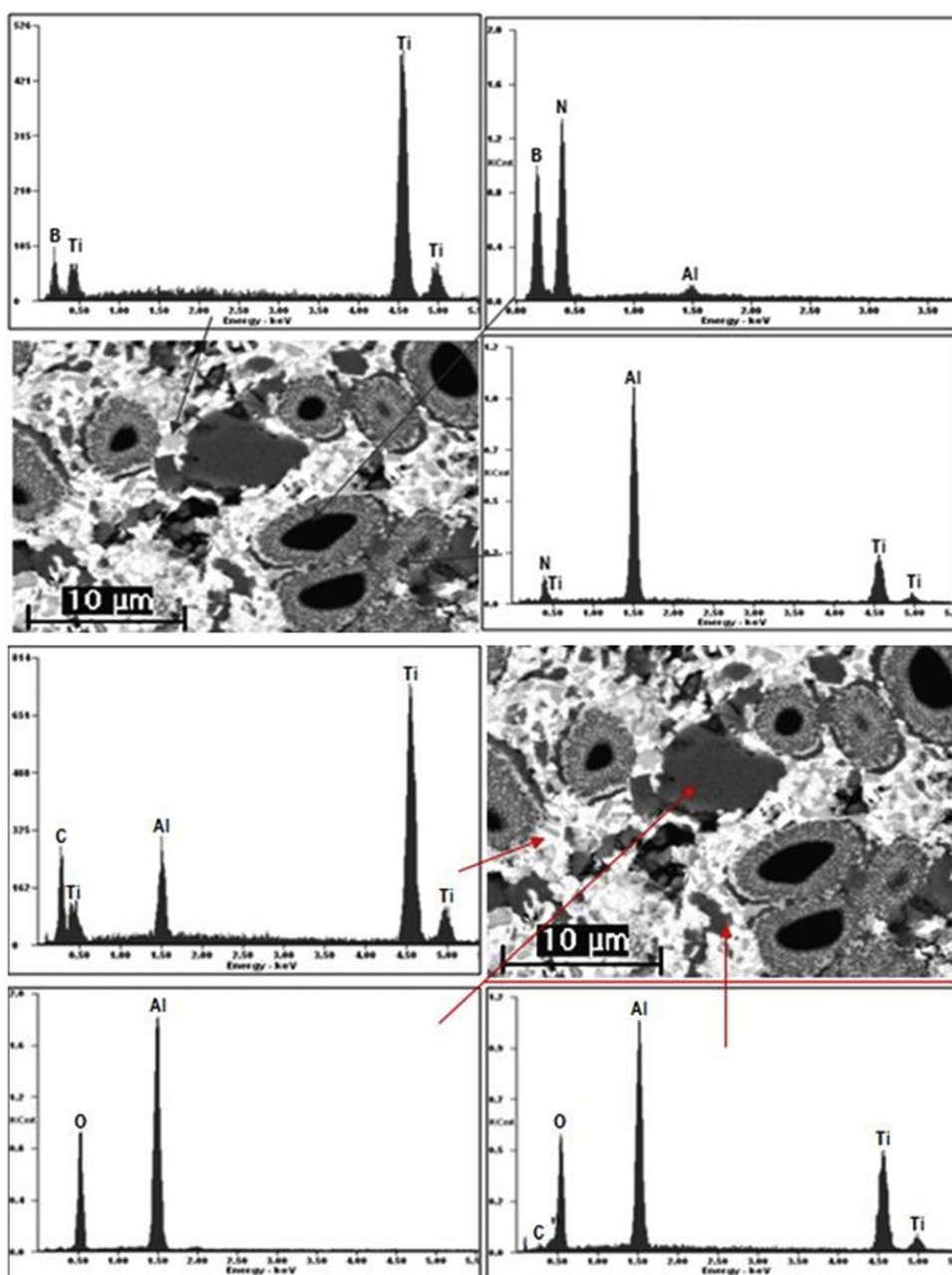


Fig. 9. SEM (SE) image at a higher magnification, and EDS analysis of $\text{Ti}_2\text{AlC}/\text{c-BN}$ composite.

in the composite materials, probably as a result of the initial high-energy crushing of MAX phase samples to form powders.

3.3.1. $Ti_2AlC/c\text{-BN}$ composites

Fig. 8 shows a SEM image of a polished cross-section of a spark plasma sintered $Ti_2AlC/c\text{-BN}$ composite. A dark black phase is seen to be dispersed in a matrix of white and dark gray; the black areas are surrounded by a light gray “rim”. Overall, the c-BN is seen to be well dispersed in the matrix.

Fig. 9 is a higher magnification SEM image, with EDS analysis, of the composite seen in Fig. 8: the black phases are c-BN as shown previously, but more detail is apparent in surrounding areas. Probable phases, based on EDS analysis and shown in parentheses, were confirmed by XRD (see Fig. 10). The light gray rim zone around the c-BN contains Ti, Al, B and N and some C ($TiAl$, TiN , TiB_2 and TiC). Similar reaction zone phases were observed by Benko et al. [13] for $TiC/c\text{-BN}$ composites, and by Rong et al. [14] for $TiN/Al/c\text{-BN}$ composites. The dark gray rim surrounding the reaction zone contains mainly Al and some Ti, N and O (AlN , TiN and Al_2O_3). The large dark gray areas in the matrix appear to be Al_2O_3 ; the lighter gray phases in the matrix contain Ti and B (TiB_2). The white phase contains Ti, Al and C and is probably the MAX phase.

Fig. 10 is an XRD diffractogram of the $Ti_2AlC/c\text{-BN}$ composite. Neither Ti_2AlC nor Ti_3AlC_2 peaks are seen: the matrix observed in Figs. 8 and 9 retains the constituent elements of the MAX phase, but has clearly decomposed. This is unlike the reaction of the bulk constituents, in which a transformation of Ti_2AlC to Ti_3AlC_2 , but not complete decomposition, was observed. The secondary phases TiB_2 , TiC , TiN , AlB_2 and AlN are identified by XRD, consistent with the EDS results. In addition to the c-BN particles, Al_2O_3 is also observed—this is probably contamination from the milling balls and from the graphite sheets used in the SPS.

3.3.2. $Ti_3SiC_2/c\text{-BN}$ composites

Fig. 11 shows a SEM image of a polished cross-section of a spark plasma sintered $Ti_3SiC_2/c\text{-BN}$ composite. The microstructure is similar to the $Ti_2AlC/c\text{-BN}$ composite: a black phase, surrounded by a light gray phase “rim”, is seen to be dispersed in a matrix of white and dark gray. Overall, the c-BN is seen to be well dispersed in the matrix.

Fig. 12 is a higher magnification SEM image of the same specimen, showing more detail, with EDS analysis. The postulated phases were confirmed by XRD. The black phases are c-BN and the light gray rim around them is the reaction zone containing Ti, Al, Si, N and O (TiN , $TiSi_2$, Al_2O_3). Similar interfacial phases were reported by Benko et al. [13] for $Ti_3SiC_2/c\text{-BN}$ composites synthesized at high pressure. The larger dark gray phases in Fig. 11 are Al_2O_3 ; the small, lighter gray phases contain Ti and B (TiB_2). The matrix consists of a white phase containing Ti, Si, C, Al

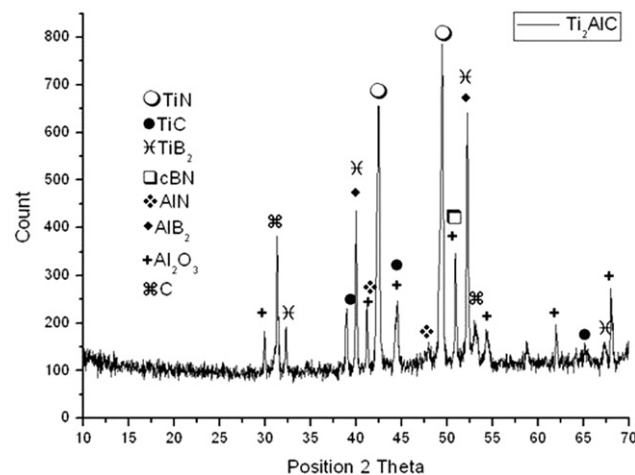


Fig. 10. X-ray diffractogram of the $Ti_2AlC/c\text{-BN}$ composite.

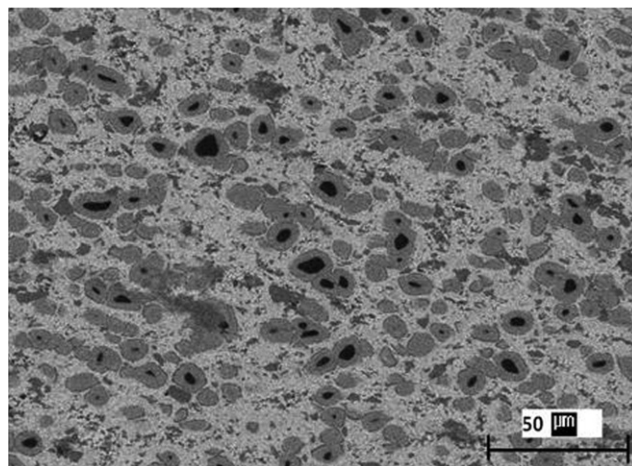


Fig. 11. SEM (SE) image of $Ti_3SiC_2/c\text{-BN}$ composite.

and B; and a dark gray phase containing Ti, Si, C, Al and O. XRD analysis shows that these are Ti_3SiC_2 with possible decomposition products ($TiSi_2$, TiC) and secondary phases.

Fig. 13 is an XRD diffractogram of the $Ti_3SiC_2/c\text{-BN}$ composite. Ti_3SiC_2 peaks are present, unlike the bulk reaction couple which showed a complete decomposition of Ti_3SiC_2 . In addition to the MAX phases and c-BN, secondary phases TiB_2 , TiC , TiN and $TiSi_2$ are observed, consistent with the EDS results. Also observed is some h-BN which may have formed from minor transformation of c-BN; remaining background peaks are possibly due to texturing of the MAX phase layered material.

3.3.3. Fracture surfaces

Fig. 14 shows the fracture surface of a $Ti_2AlC/c\text{-BN}$ composite. Three microstructural regions may be observed: dark particles of c-BN without a reaction zone on the exposed surface (A); protruding c-BN with a reaction zone remaining around it (B); and the surrounding matrix, showing a rough surface characteristic of

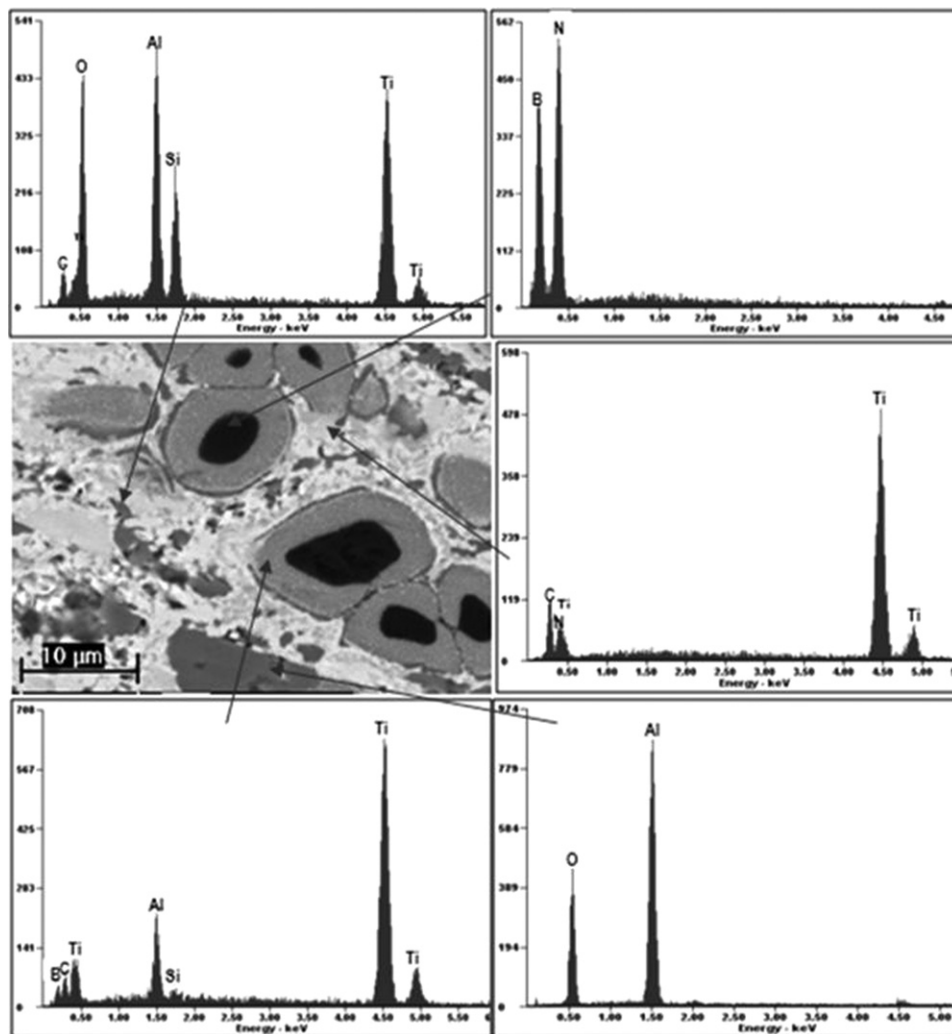


Fig. 12. SEM (SE) image with EDS analysis of $\text{Ti}_3\text{SiC}_2/\text{c-BN}$ composite at higher magnification.

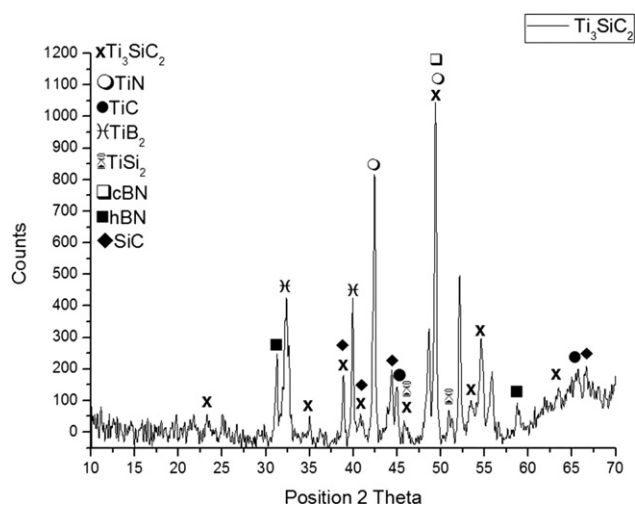


Fig. 13. X-ray diffractogram of the $\text{Ti}_3\text{SiC}_2/\text{c-BN}$ composite.

ductile fracture (C); a grain with a platelet structure is also seen. The fracture event accordingly appears to have separated some c-BN particles from the reaction region

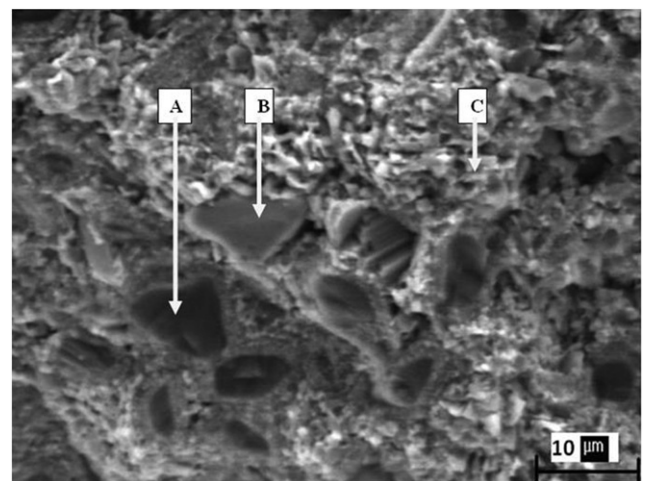


Fig. 14. SEM (SE) image of $\text{Ti}_2\text{AlC}/\text{c-BN}$ composite fracture surface.

rim (A), and elsewhere the fracture appears to have been deflected around the rim (B).

Fig. 15 shows the fracture surface of a $\text{Ti}_3\text{SiC}_2/\text{c-BN}$ composite. The same three types of microstructural region

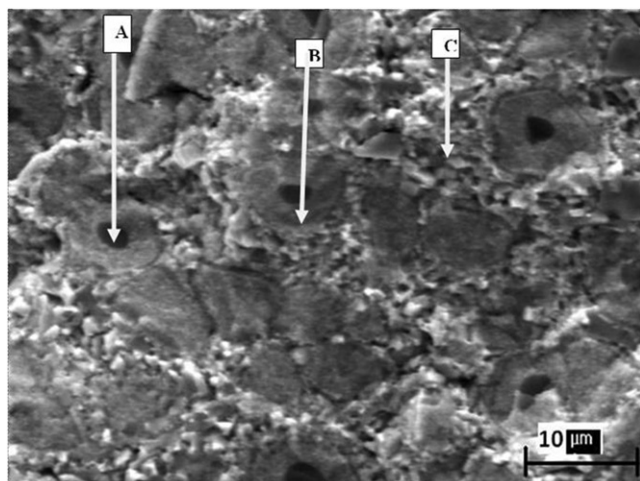


Fig. 15. SEM (SE) image of $\text{Ti}_3\text{SiC}_2/\text{c-BN}$ composite fracture surface.

may be observed: c-BN particles with no reaction region on the exposed surface (A); c-BN with a reaction region remaining (B); and a rough surrounding matrix (C), with no evidence of a platelet morphology. The fracture appears to have stripped some c-BN particles from the reaction region rim (A), and elsewhere to have been deflected around the rim (B).

The reaction zone in each composite type is bonded well with both the c-BN and the matrix, as observed from the crack which travels through the carrier phase as well as around the c-BN interface/matrix region, and also between the interface and the c-BN. This fractography shows that the c-BN particles deflect cracks in the matrix, which is expected to improve the toughness of the composite material relative to the monolithic matrix.

4. Discussion

We have synthesized composite materials in which c-BN particles are uniformly dispersed in a matrix of sintered MAX phase. This is expected to result in a material which exploits the high hardness of c-BN and the ductility of the MAX phase, to exhibit superior strength and fracture toughness. The mechanical behavior of the synthesized composites is consistent with these properties—cracks are deflected around the c-BN particles—suggesting that these materials have superior fracture toughness, and are hence outstanding candidates for cutting and grinding applications. The carrier materials; however, which started as single (MAX) phase powders, underwent some decomposition (complete for Ti_2AlC and partial for Ti_3SiC_2) during sintering of the composites, so that the composite matrix did not retain the phase structure of the starting MAX phase powders.

Preliminary investigation of bulk reaction couples shows that during sintering with c-BN, Ti_2AlC transformed to Ti_3AlC_2 , and Ti_3SiC_2 decomposed to a mixture of TiC and SiC . Processing conditions were nevertheless determined under which the transformed materials bonded well with c-BN, forming a uniform reaction zone. EDS

analysis of the reaction zones did not show the presence of any Al, indicating that the c-BN minority phases (AlN and AlB_2) did not take part in the reaction.

The composite materials, synthesized under the temperature and pressure conditions optimized for bulk reaction couples, but sintered for shorter times using SPS, exhibited c-BN particles, surrounded by an interfacial zone, well-distributed in the matrix. The chemical composition of the interfacial zone demonstrated that interaction between the c-BN and the matrix had taken place.

Ultimately two composite materials were produced from Ti_2AlC (M_2AX phase) and Ti_3SiC_2 (M_3AX_2 phase) powders. Only the $\text{Ti}_3\text{SiC}_2/\text{c-BN}$ composite retains MAX phase as the carrier phase. It appears that the shorter SPS sintering times were beneficial for retention of the Ti_3SiC_2 , M_3AX_2 phase; but promoted decomposition of the Ti_2AlC , M_2AX phase.

5. Conclusions

- Sintered MAX phases, Ti_2AlC and Ti_3SiC_2 , can be successfully reacted with bulk c-BN. The optimum conditions are 1500°C (Ti_2AlC) or 1400°C (Ti_3SiC_2), with 10 MPa pressure, for 30 min. These conditions produce defect-free reaction zones containing TiN , TiB_2 and secondary phases. Transformation or decomposition of the MAX phase was observed to occur; nevertheless these conditions proved very effective in synthesizing MAX phase/c-BN composite materials.
- MAX phase/c-BN composites were successfully produced with good adhesion of the reaction zone to both the matrix and the c-BN; at relatively low temperatures and pressures compared to previous work. Characterization of fracture surfaces shows that favorable mechanical behavior is exhibited by the composite materials, which accordingly present outstanding potential as cutting and grinding materials.

Acknowledgments

The financial support of Element six, the Department of Science and Technology and the National Research Foundation, South Africa, is gratefully acknowledged. Finally the extensive and helpful discussions with Dr. Charlie Montross, Element six, are acknowledged.

References

- [1] M.W. Barsoum, Physical properties of the MAX phases, in: K.H. Jürgen Buschow, R.W. Cahn, M.C. Flemings, B. Ilschner, E.J. Kramer, S. Mahajan, P. Veyssi re (Eds.), *Encyclopedia of Materials: Science and Technology*, Elsevier, Oxford, 2006, pp. 1–11.
- [2] I. Kero, Ti_3SiC_2 Synthesis by Powder Metallurgical Methods. Licentiate Thesis, Lule  University of Technology, 2007.
- [3] M.W. Barsoum, L. Farber, T. El-Raghy, Dislocations, kink bands and room temperature plasticity of Ti_3SiC_2 , *Metallurgical and Materials Transactions* 30A (1999) 1727–1738.

- [4] L. Vel, G. Demazeau, J. Etourneau, Cubic boron nitride: synthesis, physicochemical properties and applications, *Materials Science and Engineering B10* (1991) 149–164.
- [5] D. Akyuz, T. El-Raghy, Tools for Cutting Solid Materials. United States Patent Application Publication, US2003/186636 A1, United States of America, 2003.
- [6] M.W. Barsoum, T. El-Raghy, The MAX phases: unique new carbide and nitride materials, *American Scientist* 89 (2001) 334–343.
- [7] K. Tang, C. Wang, Y. Huang, Q. Zan, X. Xu, A study on the reaction mechanism and growth of Ti_3SiC_2 synthesized by hot-pressing, *Materials Science and Engineering A328* (2002) 206–212.
- [8] J. Qin, D. He, L. Lei, P. An, L. Fang, Y. Li, F. Wang, Z. Kou, Differential thermal analysis study of phase segregation of Ti_2AlC under high pressure and high temperature, *Journal of Alloys and Compounds* 476 (2009) L8–L10.
- [9] L. Farber, M.W. Barsoum, Isothermal sections in the Cr–Ga–N system in the 650–1000 °C temperature range, *Journal of Materials Research* 14 (1999) 2560–2566.
- [10] Y. Du, J. Schuster, H. Seifert, F. Aldinger, Experimental investigation and thermodynamic calculation of the titanium–silicon–carbon system, *Journal of the American Ceramic Society* 83 (2000) 197–203.
- [11] J. Zhu, J. Gao, J. Yang, F. Wang, K. Niihara, Synthesis and microstructure of layered-ternary Ti_2AlC ceramic by high energy milling and hot pressing, *Materials Science and Engineering A490* (2008) 62–65.
- [12] E. Benko, P. Klimczyk, S. Mackiewicz, T.L. Barr, E. Piskorska, cBN– Ti_3SiC_2 composites, *Diamond and Related Materials* 13 (2004) 521–525.
- [13] E. Benko, T.L. Barr, S. Hardcastle, E. Hoppe, A. Bernasik, J. Morgiel, XPS study of the cBN–TiC system, *Ceramics International* 27 (2001) 637–643.
- [14] X. Rong, O. Tsurumi, O. Fukunaga, T. Yano, High-pressure sintering of cBN–TiN–Al composite for cutting tool application, *Diamond and Related Materials* 11 (2002) 280–286.